Freeze-Drying

G.-W. Oetjen, Chemical Engineering, Lübeck, Germany

Introduction

Freeze-drying is a process, in which a product is first frozen and then dried by sublimation of the ice. The total process involves four steps: freezing; sublimation of the ice, called main drying (MD); desorption of the water bound to the solid, called secondary drying (SD); and packing in containers to exclude absorption of water and/or oxygen from the atmosphere. By freeze-drying a product unstable in water is transformed into a dry, stable product. The process has to be developed to satisfy four demands on the finished product: its volume remains that of the frozen substance; the structure and the biological activity of the dried solid correspond as far as possible to those of the original substance; the dried product remains stable during storage, if possible at temperatures up to $+40^{\circ}C$ and for up to 2 years; and with the addition of water the original product is quickly reconstituted. This article summarizes the problems and solutions to achieve these aims.

Theoretically, sublimation of ice can be done at atmospheric pressure; however, the vapour pressure of ice between $-10^{\circ}C$ and $-40^{\circ}C$ is approximately 2.6–0.13 mbar and 1 kg of ice has a volume of approximately $470\,m^3$ at $-10^{\circ}C$ and $8400\,m^3$ at $-40^{\circ}C$. To transport these volumes at atmospheric pressure the gas volume has to be approximately 400–8000 times larger than that of the vapour. Therefore all freeze-drying plants today are vacuum plants, in which the air is reduced to some 10% of the vapour pressure, to allow the free flow of vapour at velocities up to $100\,m\,s^{-1}$.

The first organ tissues were freeze-dried in 1890 and in 1932 a vacuum freeze-drying plant was built, but only after 1940 did it become an industrial process with the freeze-drying of blood plasma and penicillin.

Freezing

Structure of Water and Ice

In a water molecule the two H atoms form an almost tetrahedral angle with a strong dipole moment. A shell of about four water molecules exists at a distant of 28 nm, followed by a second at approximately 45 nm, and beyond 80 nm no shell can be identified. In addition to this short range order, a network of hydrogen bonds exits with a very short lifetime of 10^{-12} to 10^{-13} s.

In sub-cooled, very pure water the nucleation of ice crystals (homogeneous nucleation) starts around $-41^{\circ}C$. Normally water contains about 10^6 particles which act as nuclei for crystallization (heterogeneous crystallization). They become more effective as their structure approaches that of ice. Ice crystals exist in nine forms, of which the cubic and hexagonal at under atmospheric pressure. The growth rate of crystals depends on the diffusion of molecules to the nuclei, on finding a suitable place, and on the transportation of the freed energy to the heat sink. With extreme cooling rates (of the order of $10^5{}^{\circ}C\,min^{-1}$), crystallization can be avoided and water solidifies into an amorphous, glass-like phase. **Figure 1** shows that the amorphous phase of ice is only stable below $-160^{\circ}C$; in the range $-160^{\circ}C$ to $-130^{\circ}C$ amorphous and cubic phases can exist, and between $-130^{\circ}C$ and $-65^{\circ}C$ all the forms can be present, depending on the speed of warming. It is technically impossible to cool pure water quickly enough, to produce glassy ice; even small droplets (1 mm) injected into liquid nitrogen may freeze at a rate less than $10^3\,^{\circ}C\,min^{-1}$. The freezing behaviour of water changes completely if other substances are present in the water, e.g. cryoprotective agents (CPAs). The most widely used CPAs are:

- protein: human serum albumin, gelatin
- amino acids: glycine, arginine, alanine
- alcohols: mannitol, polyethylene glycol (PEG)
- carbohydrates
  - monosaccharides: glucose, fructose
  - disaccharides: lactose, maltose, sucrose, trehalose
- polysaccharides: dextran, cyclodextrins
- others
  - metals
  - surfactants
  - polymers
  - buffer salts

They all protect in one way or another, alone or in combination, the original quality of the product to be freeze-dried.

As an example of a CPA the influence of glycerol concentration is shown on the right-hand side of **Figure 1**. The temperature of homogenous nucleation

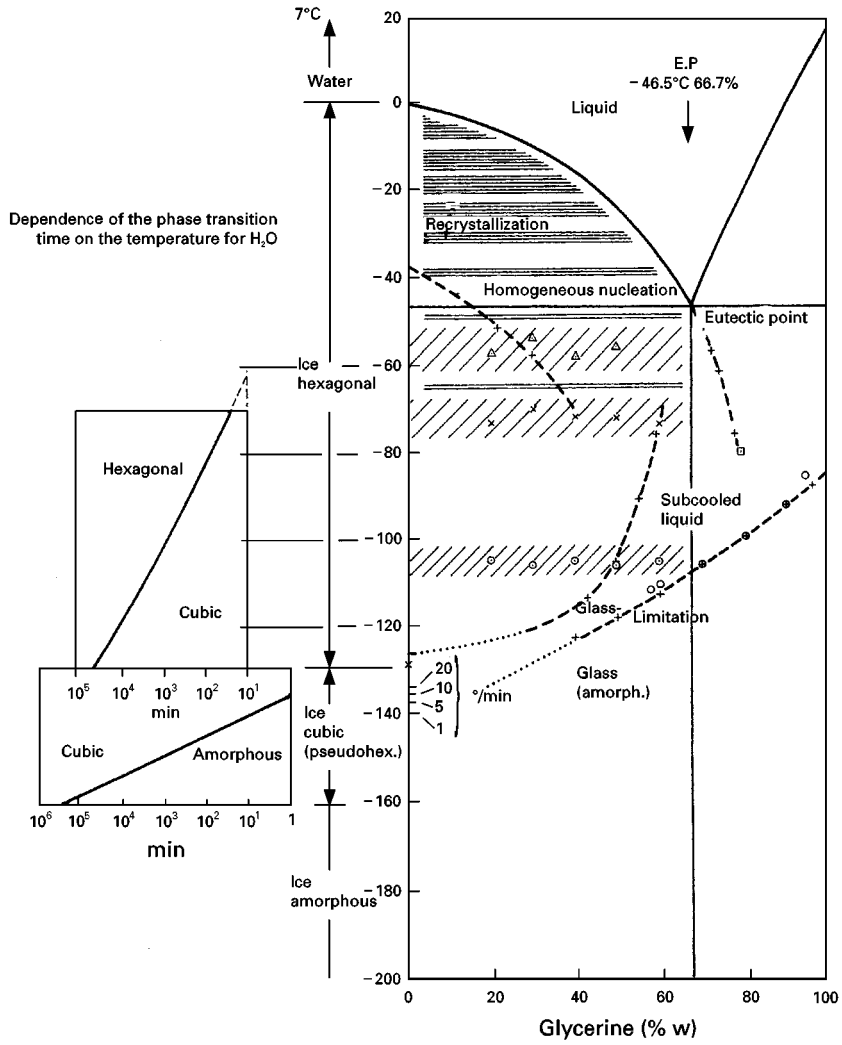

Figure 1 Phase diagram, water–glycerine. On the left-hand side the dependence of the phase transformation time from the ice temperature is shown: at −140°C amorphous ice transforms into cubic ice in approximately 10 min. (From Umrath, W. Kurzbeitrag für die Tagung Raster-Elektronenmikroskopie in Medizin und Biologie, unpublished, Brühl.)

(T_{hn}) can be reduced by about 20°C, the devitrification temperature (T_g) can rise by almost 35°C and sub-cooled liquids can exist down to very low temperatures. Polyvinyl pyrrolidone reduces T_{hn} only a few degrees, while T_g can be changed by more than 70°C. The freezing of a product is mostly done so quickly that no equilibrium state is reached during the process. The structure of the frozen product depends therefore not only on its components but also very much on the freezing rate and the temperature at the end of the freezing process. Generally speaking, during slow freezing the nuclei have time to grow and the solution in between the ice crystals becomes increasingly concentrated. During quick freezing only small crystals can grow and the remaining solution can become so viscous that the water molecules cannot diffuse to the crystals and they become part of the solidified liquid (glass) between the ice crystals.

The freeze concentration may, among other effects, change the pH, the water structure around proteins and extract water from cells. The unfrozen water will crystallize during warming when the mobility of the molecules is sufficiently increased. The crystallization can be very abrupt, warm the surroundings, melt it at least partially and destroy the structure. The freezing of a product is as critical as the drying – in some respects even more so. The structure achieved during freezing and solidification determines the main and secondary drying process, the reconstitution of the dried product and its storage capability. Therefore it is mandatory to analyse the

formation of the structure and the factors which influence it.

Methods of Structure Analysis

A number of methods have been described to supply information during freezing. Electrical resistance during cooling and warming (ER) is measured in a test vial at different freezing and warming rates. For a more accurate interpretation of the function log (ER) = $f(T)$ the first derivative of the plot is calculated as shown in **Figure 2**. The advantages of the method are: sample size is of the order of a product in a vial; it simulates heat transfer from the shelf to the vial/product; and the equipment is relatively inexpensive and easy to operate. The disadvantages are that interpretation needs some experience, the measured data reflect the mobility of ions and the amount of energy used or freed during an event cannot be calculated. In **Figure 2**A, the heat transfer medium and product are at a similar temperature; in **Figure 2**B, the wall of the test vial is isolated from the heat transfer medium to simulate the freezing of a product in a vial on the shelf. In **Figure 2**A, the effect of subcooling during freezing can be seen at about $-10°C$, but the derivative shows it more clearly between $-3°C$ and $-10°C$. During warming at event 1 ($-12°C$) the structure softens, allowing unfrozen water to crystallize, represented by the increase in resistance. In **Figure 2**B the crystallization energy cannot be quickly removed: freezing occurs in two steps. During warming, events 1 and 2 are not found, all freezable water is crystallized during cooling.

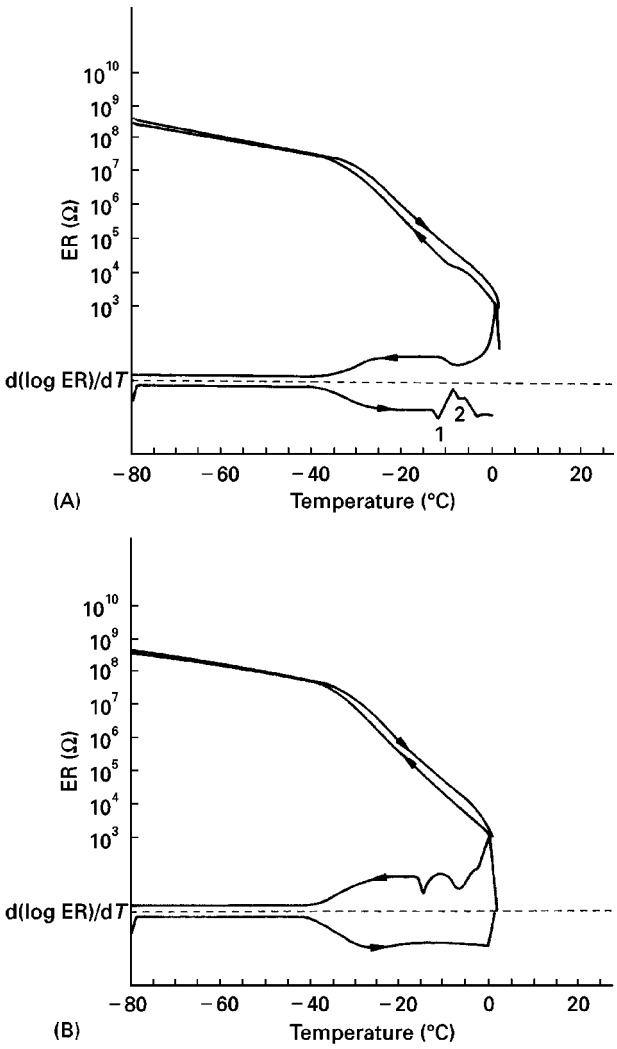

Figure 2 (A) Electrical resistance (ER) of a pharmaceutical product as a function of temperature during cooling at $1°C\ min^{-1}$ and warming at $3°C\ min^{-1}$. Heat transfer medium and product are approximately uniformly heated. (B) Measurement of the electrical resistance as in A, but with the wall of the vial insulated by a plastic tape up to the filling height of the product. Heat is therefore mostly removed through the bottom of the vial. (A and B from Willemer, H., Köln, unpublished measurements.)

Differential scanning calorimetry (DSC) compares heat flows, one to and from the sample and the other to and from a substance with no transitions in the measuring range. Roos and Karel showed by DSC (**Figure 3**) the influence of unfrozen water on T_g of fructose (1) and glucose solutions (2). After rapid freezing ($30°C\ min^{-1}$) to $-100°C$ T_g of fructose and glucose is at $-88°C$ and $-84°C$ respectively; at $-48°C$ and $-44°C$ respectively the unfrozen water crystallizes, followed by the melting of ice. If the products are thermally treated or annealed (after freezing the product is warmed to $-48°C$ for 15 min and then cooled again to $-100°C$), T_g, called $T_{g'}$ if all freezable water is frozen, is raised to $-58°C$ and $-57°C$ and no crystallization event is measurable. Time and temperature of annealing must be carefully determined to achieve a certain mobility of the molecules without collapse of the structure (see Figure 9B). The advantages of DSC are the quantitative measurement of the changes in the heat capacity of the sample and the energy freed or used in an event. The disadvantage is the small sample (milligrams), which can behave differently from a product in vials (grams) and the cost of the equipment.

In a cryomicroscope the sample can be optically observed during cooling and warming at different rates. Some models also permit freeze-drying of the sample. Willemer has shown (**Figure 4**) the structure of a Factor VIII solution during warming after quick freezing. This product must be freeze-dried at a temperature of the sublimation front of the ice (T_{ice}) below $-44°C$ and if annealing is necessary it may be possible at $-43°C$ to $-42°C$ for several minutes but a longer time at $-45°C$ is recommended. The advantage is the visual confirmation of data gained by

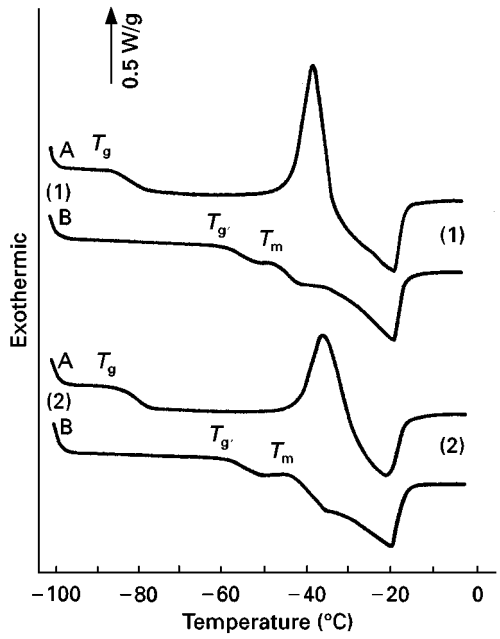

Figure 3 Results of annealing (thermal treatment) on the formation of ice in a 60% fructose solution (1) and in a 60% glucose solution (2). Curve A: after cooling at 30°C min^{-1} down to −100°C, the DSC plots have been recorded during warming at 5°C min^{-1}. T_g approximately −85°C and −88°C, respectively, for fructose and glucose. At approximately −48°C and −44°C respectively, ice crystallization starts clearly, followed by the beginning of the melting of ice. (During freezing only a part of the water has been crystallized.) Curve B: after cooling down to −100°C, the product has been warmed at 10°C min^{-1} to −48°C, kept for 15 min at this temperature (thermal treatment), cooled down again at 10°C min^{-1} to −100°C, and the DSC plot (B) measured during rewarming. During thermal treatment all freezable water is crystallized, and $T_{g'}$ is increased to −58°C and −57°C, respectively. During warming, no crystallization can be detected. (Reproduced with permission from Roos and Karel, 1991.)

other methods, e.g. ER or DSC, and the possibility to analyse the image quantitatively by computer. The disadvantages are high cost and the relatively small region of the sample that can be observed.

Nuclear magnetic resonance (NMR) provides information, among other things about free or bound water (e.g. to protein molecules), the influence of unfrozen water on the collapse temperature and the crystallization of amorphous dry products. Hanafusa has shown by NMR (**Figure 5**) how the amount of unfrozen (bound) water in a 0.57% ovalbumin solution is reduced by the addition of a 0.01 M solution of sucrose or glycerol. Similar information can be gained for a coffee extract with 25% solids: during freezing and rewarming at −70°C 0.01 g water per gram solid are unfrozen, at −40°C 0.1 g per gram and at −20°C approximately 30%; thereafter the amount increases rapidly. This extract has to be freeze-dried at a $T_{ico} < -20$°C, otherwise the structure would collapse. The unique advantage of NMR is the ability to discriminate between free, crystallized and bound water.

More details concerning these methods and additional procedures have been reported by Oetjen.

Freezing Rates

The freezing time can be estimated by an equation developed by Steinbach:

$$t_f = \Delta J/\Delta T\, \rho_g(\sigma^2/2\lambda_g + d/K_{su})$$

where t_f = freezing time; ΔJ = enthalpy difference between the initial freezing point and the final temperature; ΔT = difference of temperature between the freezing point and the cooling medium; d = thickness of the product parallel to the direction of prevailing heat transfer; ρ_g = density of the frozen product; λ_g = thermal conductivity of the frozen product; and K_{su} = surface heat transfer coefficient between cooling medium and the freezing zone.

In this equation K_{su} has to be measured for each type of vial or tray used. The flatness of the bottoms

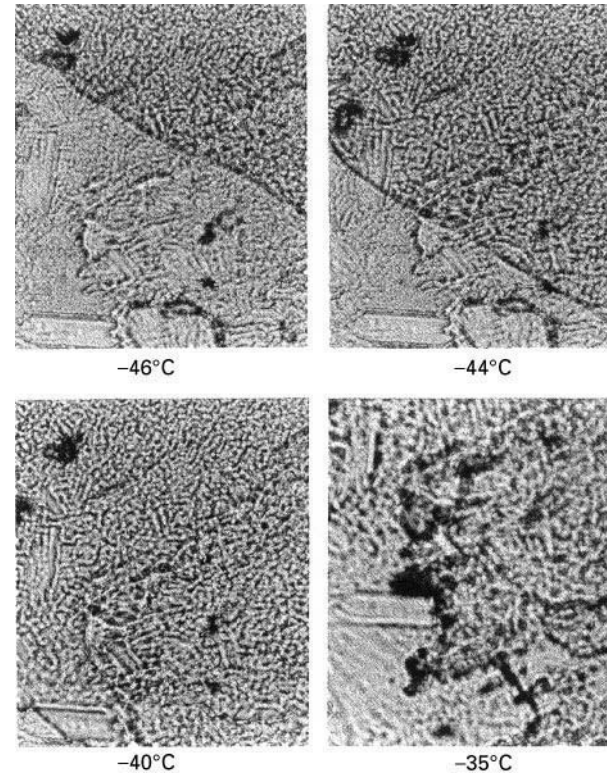

Figure 4 Photographs taken with a cryomicroscope of Factor VIII solutions at four temperatures. At −40°C the structure is still visible, but is more coarse compared with the appearance at −44°C. At −35°C the structure is collapsed. (Reproduced with permission from Willemer, 1996.)

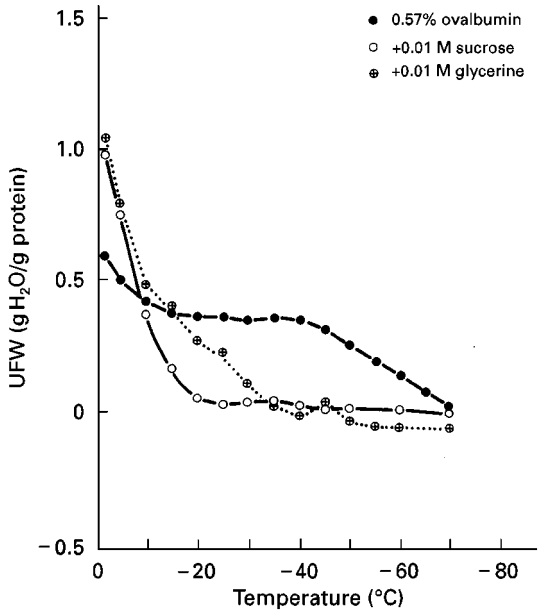

Figure 5 Unfreezable water (UFW) in a 0.57% ovalbumin solution as a function of the freezing temperature with different CPAs. (Reproduced with permission from Hanafusa, 1992.)

can change K_{su} by a factor of two – if the vials are in trays without machined bottom surfaces by a factor four and more. With K_{su} measured, t_f can be estimated with an error of 10–15%.

Main or Sublimation Drying

The main drying process (MD) has been photographed in a cryomicroscope by Kochs *et al.* as shown in **Figure 6**. The ice crystals grow extremely uniformly using a special freezing method. The ice sublimes and the remaining solids show their original structure after freezing. During sublimation the temperature of the ice at the sublimation front (T_{ice}) has to be kept well below the collapse temperature T_c.

As can be seen in **Figure 6** T_{ice} cannot be measured by a sensor because the ice front travels. If the valve between chamber and condenser (8 in Figure 11) is closed for a short time (< 3 s) the water vapour pressure in the chamber rises until the saturation pressure (ρ_g) of the ice front is reached. The rising pressure is measured 100 times per second and the change in the slope (after 2.14 s), if saturation is reached, is determined as 0.286 mbar, corresponding to $-32.7°C$ as shown by Haseley and Oetjen in **Figure 7**. This procedure is called barometric temperature measurement (BTM). It permits checking T_{ice} during MD (e.g. every 10 min). To estimate the main drying time (t_{MD}) the following equation developed by Steinbach is used:

$$t_{MD} = (\rho_g \xi_w \, LS \, \Delta m \, d)/T_{tot}\{(1/K_{tot}) + (d/2.\lambda_g) + (d/2 \, LS \, b/u)\}$$

where ρ_g = density of the frozen product (kg m^{-3}); ξ_w = amount of water (kg kg^{-1}); LS = sublimation energy (2.805 kJ kg^{-1}); T_{tot} = temperature difference ($T_{sh} - T_{ice}$); K_{tot} = total heat transmission coefficient from the shelf to the sublimation front of the ice; λ_g = thermal conductivity of the frozen product; d = thickness of the layer (m); Δm = content of frozen water; and b/μ = permeability (kg m^{-1} h^{-1} mbar^{-1}) for water vapour through the dried product.

T_{tot} is known, if T_{ice} is measured and K_{tot} has to be measured once for each type of container; one can

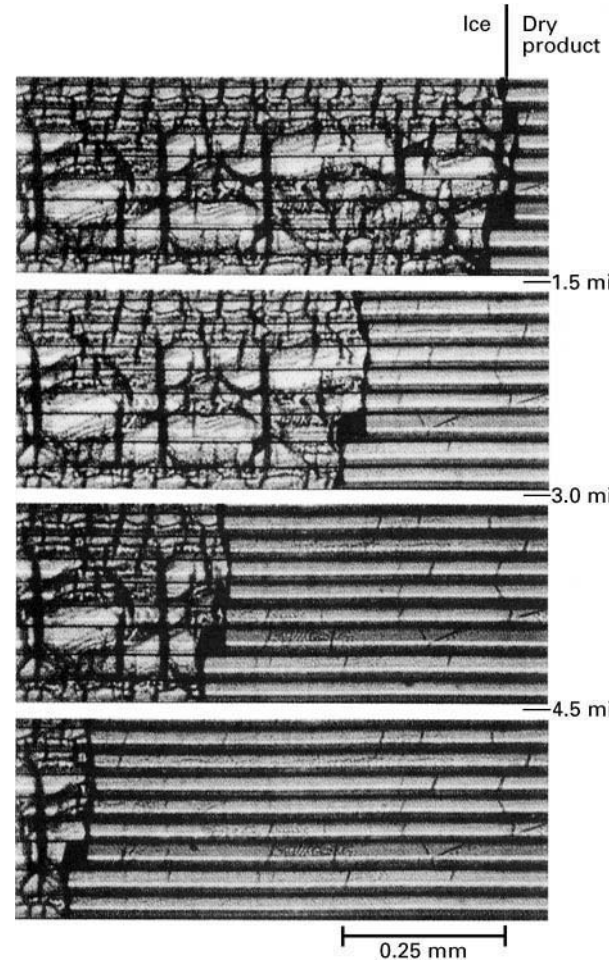

Figure 6 Course of main drying observed using a cryomicroscope, in which freeze-drying is carried out. The hydroxyethyl starch solution is optimally frozen. The dark lines show the form of the sublimated ice crystals. (Reproduced with permission from Kochs *et al.*, 1991.)

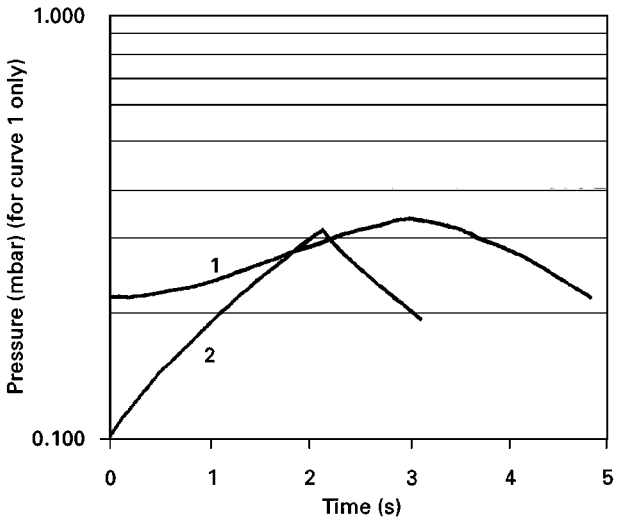

Figure 7 Pressure rise as a function of time. 1, Pressure rise in the chamber after the valve is closed; 2, first derivative of 1. The maximum of 2 is reached at 2.14 s; the related equilibrium vapour pressure $p_s = 0.286$ mbar, corresponding to $T_{ice} = -32.7°C$. (Reproduced with permission from Haseley and Oetjen, 1998.)

expect values between 60 and 120 kJ m^{-2} h^{-1}°C^{-1}. K_{tot} is only slightly dependent on the operation pressure up to 0.1 mbar; then it increases up to 1 mbar by a factor of two. λ_g is, in most cases, the figure for pure ice. Δm has to be determined for each product by methods described above. $b/\mu = 1.3 \times 10^{-2}$ (kg m^{-1} h^{-1} $mbar^{-1}$) is an average which is often found in practice, it can vary by a factor of two, but

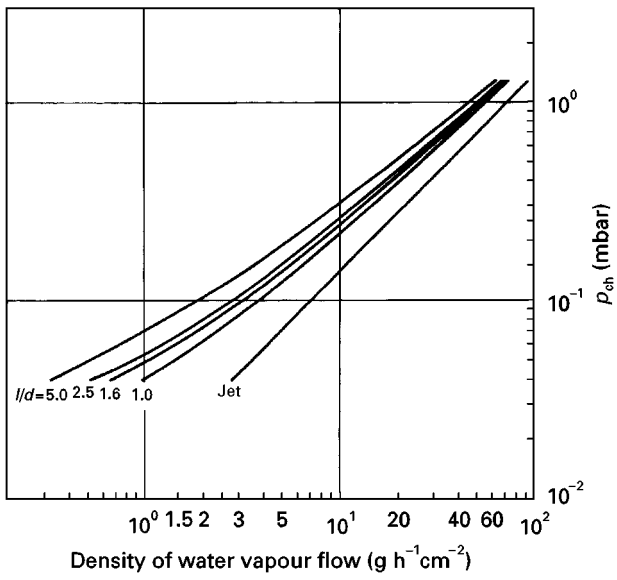

Figure 8 Density of water vapour flow (g cm^{-2} h^{-1}) as function of p_{ch} with jet flow and different l/d as parameter. (Reproduced with permission from Oetjen, 1999.)

the term with b/μ in most freeze-drying processes only has an influence of a few per cent on t_{MD}. The standard deviation of T_{ice}, measurements during MD in the range of -15 to $-45°C$ should be $< 0.5°C$, if measured automatically. t_{MD} is in most cases governed by the value of T_{tot} and the term $(1/K_{tot})$. The term $(d/2 \cdot \lambda_g)$ is, for d values below 10 mm, of the order of 10% or less of l/K_{tot}, growing to approximately 50% at $d = 35$ mm. T_{ice} is the result of a thermodynamic equilibrium between heat transfer to the sublimation front and energy consumption for sublimation. Both depend on several factors, but the heat supply and vapour transport to the condenser are most important during MD. Therefore the operation pressure is a very effective tool to control T_{ice}, if the shelf temperature is kept constant and the condenser temperature is always below a maximum, which depends on the water vapour pressure in the chamber and the design of the plant. By changing the operation pressure, e.g. from 0.1 mbar to 0.8 mbar, T_{ice} can be controlled between $-30°C$ and $-20°C$. For another product, a different product thickness or a different plant, the pressure range and its controlled range are different, but the dependence is reproducible. Since T_{ice} depends also on the structure of the frozen product it can be used to prove that the structure of products in different runs is homogeneous and sufficiently identical. If the structure contains unfrozen water, T_{ice} data will from time to time jump by 1°C or more (when the water evaporates) and the data will be different for a product frozen at different freezing rates.

At the end of MD the ice is mostly sublimed and the measured T_{ice} decreases below the standard deviation of T_{ice} during MD. This effect can be used to change automatically from main to secondary drying (SD), e.g. if the measured T_{ice} becomes 2–3°C smaller than the average during MD. Other criteria are often suggested, such as an increase of product temperature, a decrease in operating pressure or a decrease in partial pressure of water vapour, but it is more difficult to use these other methods quantitatively.

Besides heat transfer, the water vapour transport from the chamber to the condenser is often critical in a freeze-drying process. The length (l) and diameter (d) of the connection between chamber and condenser in a freeze-drying plant as shown in Figure 11 determine the vapour flow, assuming that the other flow resistances in the chamber are relatively small by comparison. The vapour flow can be estimated using the Günther–Jaeckel–Oetjen equation. **Figure 8** shows that: the vapour flow density decreases in a nonlinear manner with the chamber pressure; the relation of l/d is of increasing importance with decreasing pressure; for example, at 4×10^{-2} mbar the vapour

flow density at $l/d = 5$ is only 30% that at $l/d = 1$. Right-angle bends contribute to the length not only by their physical dimensions but, depending on the design, by a factor of four or more of the measured length. For operation pressures below about 10^{-1} mbar, $l/d > 2.5$ should be avoided.

Secondary or Desorption Drying

Desorption Rates

During secondary drying (SD), water that is removed is more less bound to solid molecules. The amount of water removed is small (e.g. 10% of solids), compared to 10 times the weight of solids during MD. The behaviour of water molecules close to a protein surface has been described by Bellissent-Funel and Teixeira. The water molecules are in a monolayer around the protein with a reduced mobility compared with bulk water.

The desorption of bound water can be measured during SD by measuring the pressure rise in the chamber after closing the valve to the condenser for 60–120 s. The length of time is not critical since the temperature does not change quickly in this phase. The pressure rise ($dp\ s^{-1}$) can be converted into the desorption rate (DR) using:

$$DR = 2.89 \times 10^2\ (V_{ch}/m_{so})\ (dp/dt)$$

where DR = desorption of water vapour in per cent of solids per hour; V_{ch} = chamber volume (L); dp = pressure rise (mbar); dt = time of dp (s); and m_{so} = mass of solids (g).

The course of DR describes not only the progress of the secondary drying quantitatively, but also reflects the structure of the frozen product as shown by Haseley and Oetjen in **Figure 9**. In **Figure 9**A DR data are shown for a 10% mannitol solution frozen in vials on the shelves of the freeze-drying plant at a rate of 0.5–0.8°C min^{-1}. In **Figure 9**B the same solution in the same vials is frozen in liquid nitrogen and in Figure 9C the solution is frozen in liquid nitrogen but annealed before freeze-drying. From these figures the following conclusions can be drawn. (1) Slow freezing of 10% mannitol solutions results in structures in which the water is bound in several forms. The DR plots as a function of time are not single-valued. (2) Freezing at rates of more than 30°C min^{-1} produces structures with a more uniform desorption behaviour. DR plots show the influence of the operating conditions during MD: (1) run 6 in **Figure 9**B is collapsed, and the water has dissolved part of the solids, forming a sticky cake. The water vapour of 378 vials resulted in an unstable T_{ice}, which is 5–7°C higher than in all other runs. (2) The systematic influence of T_{sh} is shown in **Figure 9**B and C. (3) The influence of p_c is shown in **Figure 9**C, and the influence of annealing or low T_{ice} is demonstrated by comparing Figure 9B and C: without annealing, DR plots bend between 3% and 5% per hour; with annealing this effect practically disappears. The exceptions prove the sensitivity of the measurements: run 1 (Figure 9B) is freeze-dried at $T_{ice} = -36.9$°C, others at approximately -34.9°C; run 5 (Figure 9B) is annealed at -40°C but for 8 h; runs 2 and 3 (Figure 9C) are annealed at a temperature 1°C too high and 1.5°C too low for 18 min. Annealing reduces the amount of unfrozen water.

Residual Moisture Content

The integration of DR over time results in the amount of water which can still be desorbed; this is called desorbable water, dW or residual moisture content. In **Figure 10** Haseley and Oetjen show the calculated plots from the DR data of Figure 9B and C. From the lower part of Figure 10, it follows that the heat conductivity of the annealed product during SD is almost 100% higher and more uniform than that of the unannealed product. The upper part shows that the correctly treated products and the one dried at a low T_{ice} during MD will dry more quickly than the others.

Storage

The storage capability of a dried product depends generally on its chemical and structural qualities. The complexity of the problem is highlighted, for example, by the storage stability of therapeutic proteins. The degradation of a protein, the irreversible change in primary structure, conformation or state of aggregation in a glassy surrounding depends on the thermodynamic behaviour of the glass as well as on the qualities of the protein produced during freezing and freeze-drying, as shown by Pikal. The storage temperature of such products has to be well below T_g of the dried formulation; nevertheless unfolding or aggregation of unfolded molecules can occur because of poor interaction between the stable glass structure and movements in protein configurations. From this example some simplified guidelines can be proposed. There are no general rules to estimate the maximum storage time at a maximum tolerable temperature – both depend even on small changes in the formulation of a drug or the variations between two types of fruits or the processing methods of extracts (e.g. coffee). In many cases the maximum storage time is

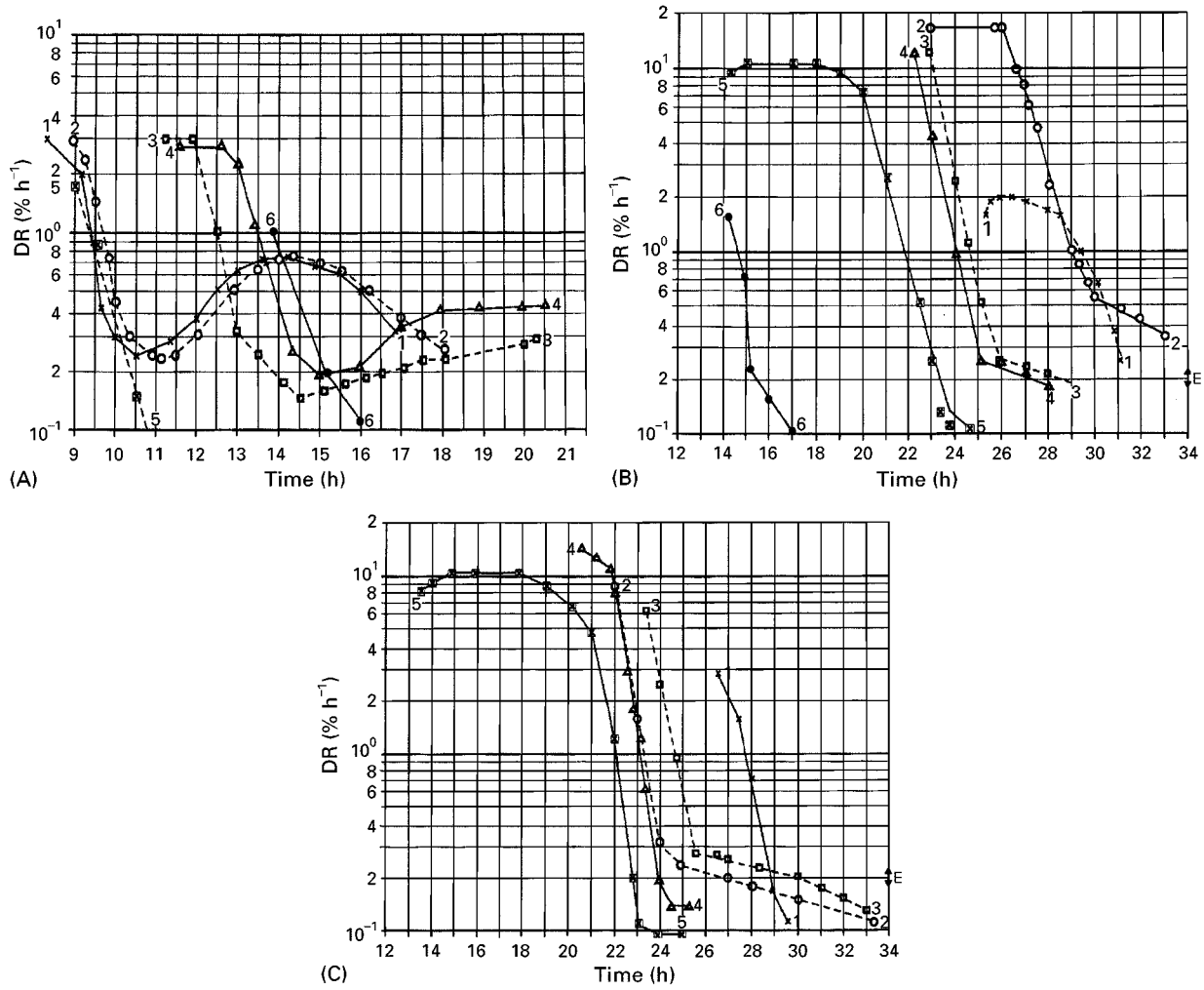

Figure 9 (A) Desorption rate (DR) as a function of time of a 10% mannitol solution frozen on the shelves of the freeze-drying plant at a rate of 0.5–0.8°C min^{-1}. In all runs: 300 vials at an operation pressure (p_c) = 0.3 mbar during MD. Runs 1 and 2 at a shelf temperature (T_{sh}) = 20°C; runs 3 and 4, T_{sh} = 5°C. Plot 5 egg albumin and plot 6 saccharose for comparison. (B) DR as in A, but the solution is frozen in liquid nitrogen at a rate between 35°C and 66°C min^{-1}. During MD all runs at p_c = 0.15 mbar, except run 1 = 0.08 mbar and T_{sh} in run 1 = −5°C; in run 2 = 0°C; in runs 3–6 = 0°C for the first 11 h, thereafter until end of MD 10°C. In runs 1–5, 126 vials; in run 6, 378 vials. Run 5 intentionally changed from MD to SD 7 h earlier than in runs 3 and 4. (C) DR as in B, but the frozen mannitol was annealed at slightly different temperatures and times:

Run	Annealing temperature (°C)	Annealing time (min)
1	−24	18
2	−23.5	18
3	−26	18
4	−24.5	18
5	−24	20

All runs at p_c = 0.15 mbar, T_{sh} in the first 11 h = 0°C, thereafter 10°C, during SD = 30°C except run 1 p_c = 0.08 mbar and T_{sh} = −5°C in the first 11 h. (Reproduced with permission from Haseley and Oetjen, 1999.)

inversely related to the maximum temperature and depends strongly on the residual moisture content (±1% or less can be decisive). For crystallized products (e.g. antibiotics) the crystal structure must not change during storage and for glassy products the maximum storage temperature has to be well below T_g (see above). The main difference between the stresses during drying and storage is the length of the

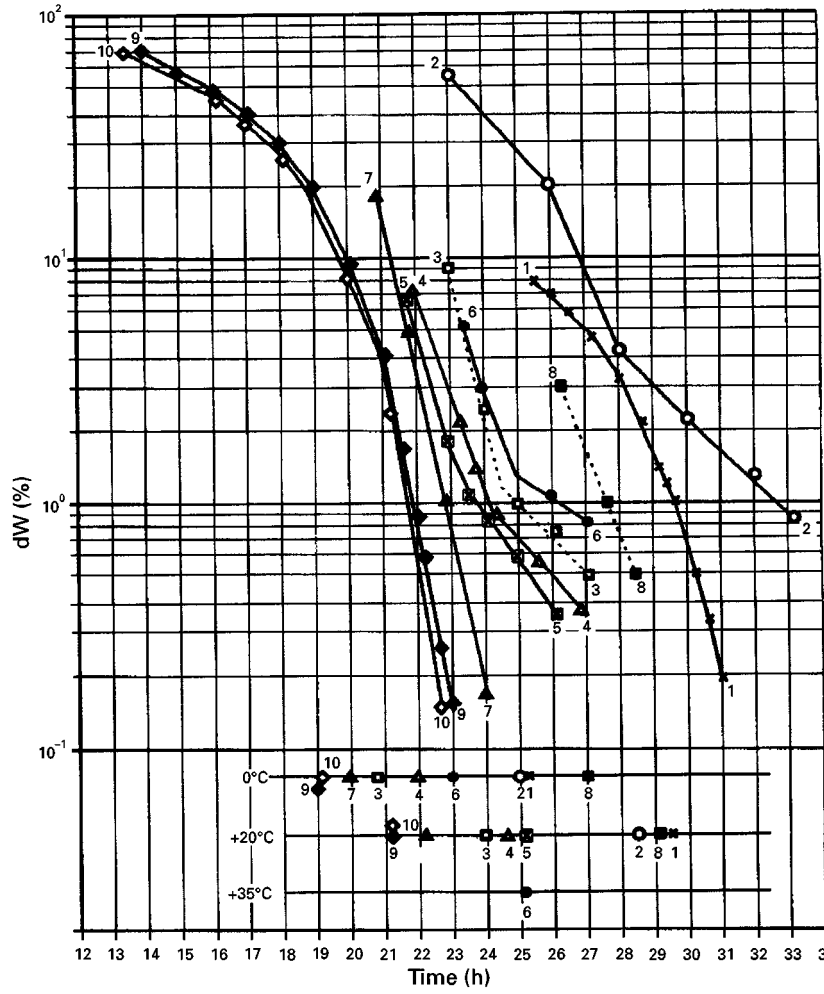

Figure 10 Residual moisture content shown as desorbable water (dW) during secondary drying. Plot 1 = plot 1 in Figure 9B; 2 = 2 (9B); 3 = 3 (9B); 4 = 4 (9B); 9 = 5 (9B); 5 = 2 (9C); 6 = 3 (9C); 7 = 4 (9C); 8 = 1 (9C); 10 = 5 (9C); except run 1, $p_c = 0.08$ mbar and $T_{sh} = -5°C$ in the first 11 h. (Reproduced with permission from Haseley and Oetjen, 1999.)

effective time: a few hours as opposed to many months up to years.

Relaxation time in molecular configurations may be large compared with the drying cycle, but this may be totally different for the long-term storage time. Besides temperature-induced changes, the residual moisture content (RM) can increase the mobility of molecules and promote chemical reactions. The RM at the end of drying can be as specified; nevertheless moisture can diffuse from the stoppers closing the vials into the product, raising the RM by several per cent during storage. Stoppers and the gas in the container of the product have to be dried carefully. On the other hand, 'the drier the better' is unjustified for many products. The Maillard reaction increases with decreasing water activity ($a_w = p/p_s$, where p = vapour pressure of the product and p_s = saturation vapour pressure) as well as the oxidation of fats. Influenza virus in a freeze-dried formulation shows the largest decrease in infectivity at 0.4% and 3.2% RM, while at 1.7% it is about 30 times less. Tissue plasminogen activator and human growth factor in certain formulations are optimally stabilized if they are surrounded by a monolayer of water molecules (which may not be distributed evenly).

Freeze-Drying Equipment

Figure 11 shows a freeze-drying plant, designed for maximum current demands. The condenser is cooled by liquid nitrogen controllable between $-70°C$ and $-100°C$ (T_{co}); the brine for the shelves is temperature-controlled (T_{sh}) between $+60°C$ and $-80°C$ (cooling by liquid nitrogen); the four-stage pump set can reach about 5×10^{-5} mbar (p_e); the vials can be closed shelf by shelf by a hydraulically operated

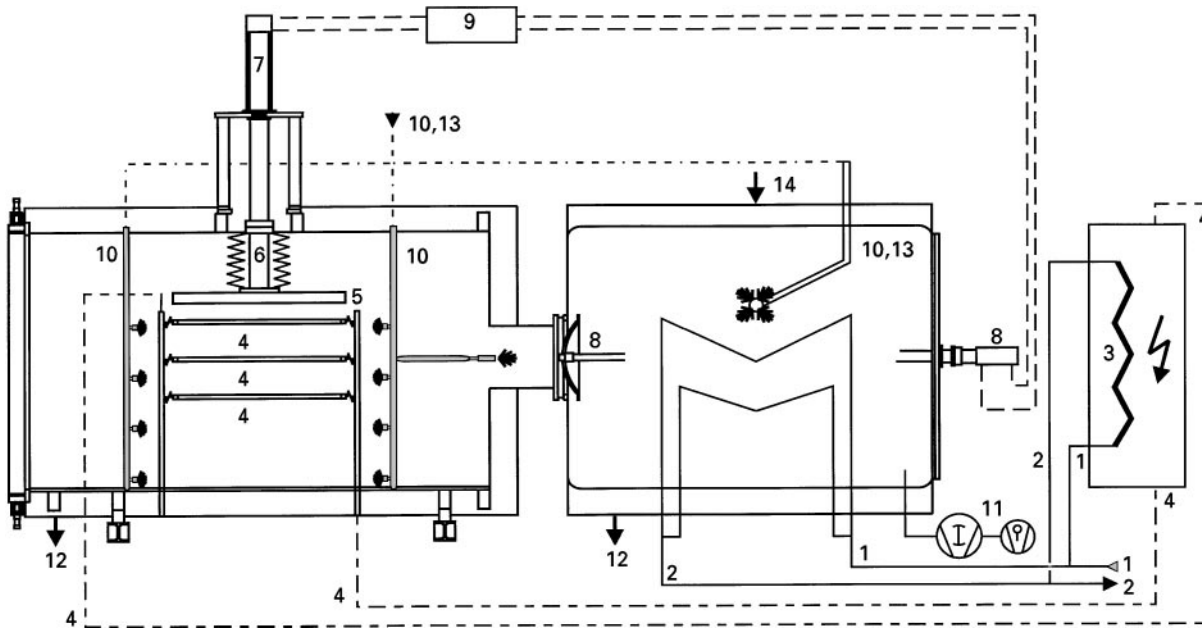

Figure 11 Freeze-drying plant condenser and shelves cooled with liquid nitrogen. Clean In Place system in chamber and condenser. 1, liquid nitogen inlet to condenser and heat exchanger; 2 nitrogen outlet from the condenser and heat exchanger; 3, heat exchanger for the brine in the shelves; 4, brine to and from the shelves; 5, pressure plate for closing vials; 6, piston rod with bellows; 7, hydraulic piston for 5 and 6; 8, hydraulically operated valve; 9, hydraulic system; 10 and 13, water and steam inlets; 11, pumping system; 12, water outlet. (Courtesy of Steris GmbH, Hürth, Germany.)

pressure plate; the connection between chamber and condenser is as short as technically possible; the valve between chamber and condenser is operated by a fast hydraulic piston; chamber and condenser can be cleaned by a pressure spray and cleaning system (clean-in-place); chamber, condenser and all components within them can be sterilized by the pressureless Vaporized Hydrogen Peroxide (VHP)® process; loading and unloading of the plant is fully automatic; the documentation and control of the total process from loading to freezing, to drying, to closing of the valves, to venting and unloading can be automatic with no thermocouples in the product; this includes the change from MD to SD, the calculation of the moisture content during SD and the termination of the secondary drying at a specified moisture content.

If no extreme temperatures are required, refrigerant compressors can be used for the condenser down to $T_{co} \approx -80°C$ and for the brine down to $T_{sh} \approx -60°C$, and a three-stage pump set is sufficient. If steam sterilization is mandatory, the equipment has to be built for pressures up to 2.5 bar and temperatures up to 125°C.

At the other end of the line of freeze-drying equipment laboratory installations are found, of which a typical example is shown in **Figure 12**. Usually the product is frozen in vials or trays in a separate freezer or in the condenser of the plant and the shelves are only heated. The chamber is often a bell jar, $T_{co} \approx -45°C$, $p_e \approx 0.05$ mbar. It is not advisable to use this type of plant as a pilot plant for process development, because the product temperature is not sufficiently uniform and cannot be controlled accurately, especially in the low temperature area.

Regulatory Issues

In the *Validation Documentation Inspection Guide*, US Department of Health and Human Services, Food and Drug Administration, 1993, process validation is defined as follows:

- Establishing documented evidence, which provides a high degree of assurance that a specific process will consistently produce a product meeting its predetermined specifications and quality attributes.
- The *Guide to Inspections of Lyophilization of Parenterals*, published by the US Food and Drug Administration, July 1993, contains among others the chapters 'Lyophilization Cycle and Controls', 'Cycle Validation' and 'Lyophilizer Sterilization/Design'.

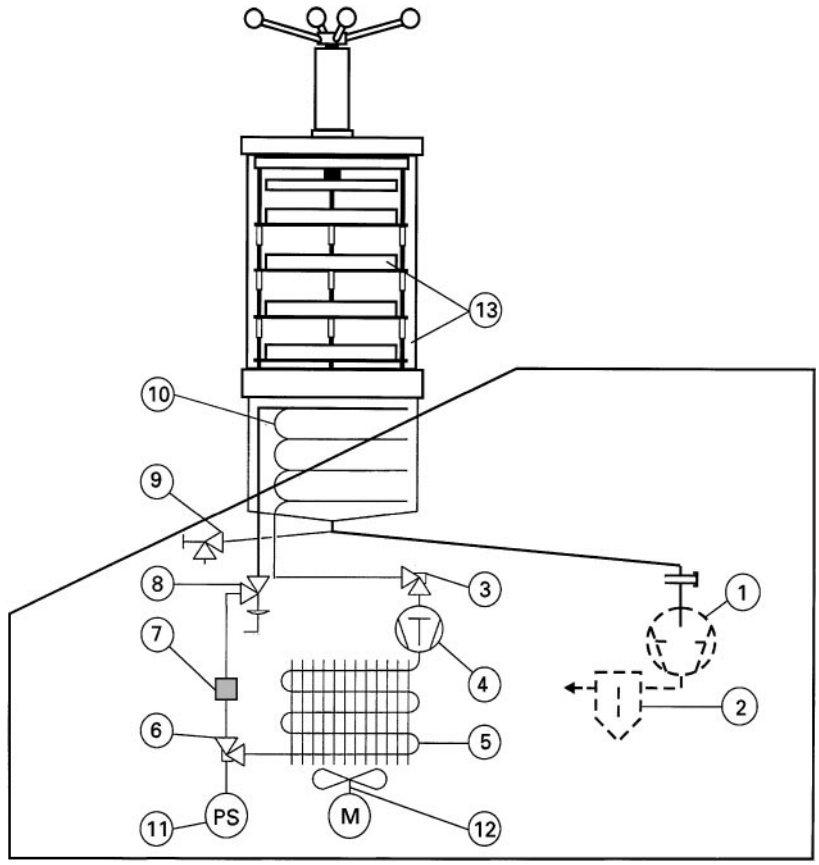

Figure 12 Schema of a laboratory freeze-drying plant: 1, two-stage vacuum pump; 2, exhaust filter; 3, valve; 4, refrigeration compressor; 5, liquefaction of refrigerant; 6, valve; 7, filter; 8, injection valve; 9, drain valve; 10, ice condenser; 11, pressure switch; 12, ventilator; 13, drying chamber with heated shelves and closing system for stopper of vials. (Lyovac® GT 2, Courtesy of Steris GmbH, Hürth, Germany.)

In the European Union, the directive 91/356 EEC provides the principles and guidelines of Good Manufacturing Practice (GMP). In a series of annexes, supplementary guidelines are covered, but up until 1996 only 'Annex 1: Manufacture of Sterile Medical Products' has been revised. In spite of all these guidelines and annexes, Monger summarized the situation for the user of freeze-drying processes and installations as follows: 'It might be expected that some substantial guidance would be provided. Regrettably, this is not so'.

Powell-Evans provided a range of advice on how to 'streamline validation', which he calls 'one of the most time-consuming and costly exercises faced by pharmaceutical manufacturers'. The qualification and validation of freeze-drying installations and processes for the production of pharmaceuticals cannot be summed up in this section. For cosmetic and food products regulatory issues, depending on the country of manufacturing and use, have also to be followed.

Conclusion

Freeze-drying is the most complex and costly conservation process of all drying methods. However, it is the only way for many pharmaceutical products to maintain their original qualities for an acceptable time at readily available temperatures or even at room temperature and above. For food and cosmetic products it provides an opportunity to supply the customers with stable high quality products which can be easily used. For many products, e.g. some antibiotics and some food ingredients, simpler methods of preservation have been developed but in pharmaceuticals there is an increase in the number of products which have to be frozen and freeze-dried at low temperatures using tightly controlled processes. The tendency to automate the whole procedure is promoted by three goals: (1) to have little or no personnel in the sterile areas; (2) to restrict the volume of sterile areas as much as possible, for example by enclosing the whole production line from vial filling to

Figure 13 (See Colour Plate 37). Isolator, Class 100, for filling, transportation and loading of vials into the freeze-drying plant. Decontamination of the isolator and the equiment therein is accomplished by vaporized hydrogen peroxide (VHP). The VHP 100® generator can be seen in the centre in front of the isolator. (Courtesy of Steris GmbH, Hürth, Germany.)

unloading from the chamber in isolators as shown in **Figure 13**; (3) to exclude human error as much as possible and to have each step documented by computer.

To automate an existing process can be more difficult than to develop a new automated process. This is based on several factors. The formulation of the drug has to reflect the automation, e.g. filling and loading can require hours, during which the solution has to be stable, possibly at room temperature. Freezing of the product on the shelves and drying in the chamber have to be executed without temperature sensors in the product; other methods of temperature control have to be used, tested and installed. Criteria have to be defined for the automatic change from main to secondary drying. Automatic termination of the secondary drying has to be effected when certain measurable events are accomplished. Besides these main points several others have to be evaluated. More accurate and independent sensor systems will influence freezing and drying procedures. The required data processing and the actuators to fulfil the commands are available today.

See Colour Plate 37.

Further Reading

Bellissent-Funel MC and Teixera J (1999) Structural and dynamic properties of bulk and confined water. In: Rey L and May JC (eds) *Freeze-Drying/Lyophilization of Pharmaceutical and Biological Products*, pp. 53–77. New York: Marcel Dekker.

Hanafusa N (1992) The behavior of hydration water of protein with the protectant in the view of HNMR. In: May JC and Brown F (eds) *Developments in Biological Standardization*, vol. 74, pp. 241–253. Basel: Karger.

Kochs M, Körber Ch, Nunner B and Heschel I (1991). The influence of the freezing process on vapor transport during sublimation in vacuum-freeze-drying. *International Journal of Heat and Mass Transfer* 34: 2395–2408.

Monger P (1997) Freeze dryer validation. In: Cameron P (ed.) *Good Pharmaceutical Freeze-Drying Practice*, p. 157. Buffalo Grove, IL: Interpharm Press.

Oetjen GW (1999) *Freeze Drying*, ch. 1.1.5. Weinheim: Wiley–VCH.

Oetjen GW (1999) *Freeze Drying*, ch. 1.2.4. Weinheim: Wiley–VCH.

Pikal MJ (1999) Mechanisms of protein stabilization during freeze-drying and storage: the relative importance of thermodynamic stabilization and glassy state relaxation dynamics. In: Rey L and May JC (eds) *Freeze-Drying/Lyophilization of Pharmaceutical and Biological Products*, pp. 161–198. New York: Marcel Dekker.

Steinbach G (1971) *Equations for the Heat and Mass Transfer in Freeze-Drying of Porous and Non-Porous Layers and Bodies*, pp. 674-683. Washington, DC: International Institute of Refrigeration.